Membrane Potential across Low-Water-Content Charged Membranes: Effect of Ion Pairing

Hidetoshi Matsumoto, Ryotaro Yamamoto, and Akihiko Tanioka*

Department of Organic and Polymeric Materials and International Research Center of Macromolecular Science, Tokyo Institute of Technology, Mail Box S8-27, 2-12-1 Ookayama, Meguro-ku, Tokyo 152-8552, Japan

Received: March 29, 2005; In Final Form: May 21, 2005

In the present paper, we systematically examined the ion-pairing effect in low-water-content charged membranes. Cation- and anion-exchange membranes with various water contents and homogeneous fixed-charge distribution were prepared by radical copolymerization and then characterized by membrane potential measurements. The experimental results were analyzed by our recently developed theoretical model (Yamamoto, R.; Matsumoto, H.; Tanioka, A. *J. Phys. Chem. B* **2003**, *107*, 10615), which is based on the Donnan equilibrium, the Nernst−Planck equation for ion flux, and the Fuoss formalism for ion-pair formation between the fixed-charge group and the counterion in the membrane. The theoretical predictions agreed well with the experimental results for both cation- and anion-exchange membranes. This supported the belief that the ion-pairing effect was substantial in a low-water-content membrane system. Our theoretical analysis also showed the following results: (i) the dielectric constant in the membrane, ϵ_r, was smaller than the value in bulk water, (ii) the center-to-center distance of the ion pair, *a*, was independent of the water content of the membranes, and (iii) the charge effectiveness of all membranes, *Q*, was small (<0.35).

1. Introduction

Recently, the application of low-water-content charged (ion-exchange or polyelectrolyte) membranes under severe conditions has become more attractive, for example, in fuel cells, the recovery of highly concentrated acids/bases, and high-temperature membrane processes for high efficiency. For these applications, the membranes require the following properties: (i) high fixed-charge density, (ii) low-volume flux generated by the osmotic pressure difference, and (iii) high thermal, mechanical, and chemical stability. The low-water-content charged membrane is a promising option.[1−3]

Ionic transport phenomena through a charged membrane are strongly affected by the fixed-charge groups in the membrane. All of the fixed-charge groups in the membrane do not function perfectly. The fixed-charge density of the membrane estimated by the ionic transport procedure (membrane potential method) is less than that by the equilibrium one (titration method).[4−6] It has been considered that this phenomenon is attributed to a decrease in the activity of fixed-charge groups in the membrane due to ion-pair formation between the fixed-charge group and the counterion in the membrane.[7−13] Mafé et al. proposed a theoretical model considering the ion-pairing effect between the fixed-charge group and the counterion in the membrane.[14] According to their model, the ion-pairing effect is more substantial under a low-dielectric-constant condition (e.g., a nonaqueous solution system or a low-water-content membrane system). Chou et al. studied the ion-pairing effect in a nonaqueous solution system and revealed that theoretical predictions agreed well with the experimental results based on the membrane potential and permeability measurements.[15−18] Our previous work indicated that the effect of ion-pair formation was substantial in low-water-content cation-exchange membranes with inhomogeneous fixed-charge distribution.[2,3] However, the ion-pairing effect in low-water-content membranes has not been verified systematically. In the present study, we prepared cation- and anion-exchange membranes with various water contents and homogeneous fixed-charge distribution by radical copolymerization and examined the ion-pairing effect based on membrane potential measurements. This is the first comprehensive study on the ion-pairing effect in low-water-content charged membranes.

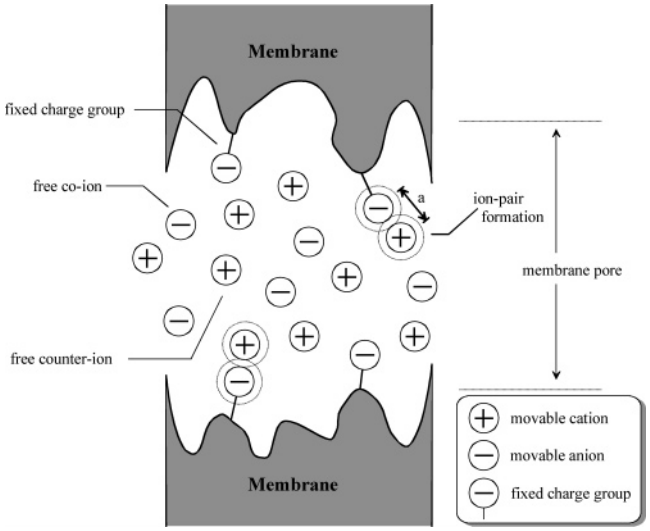

Figure 1. Simplified view of ion pairing in a negatively charged membrane.

2. Theoretical Background

2.1. Ion-Pair Formation in the Membrane. In a charged membrane, the fixed-charge groups associate with the counterions (Figure 1). To estimate the ion-pairing effect between the

* Author to whom correspondence should be addressed. Phone: +81-3-5734-2426. Fax: +81-3-5734-2876. E-mail: atanioka@o.cc.titech.ac.jp.

10.1021/jp051585s CCC: $30.25
Published on Web 06/30/2005

fixed-charge groups and counterions in the membrane phase, we adapted a simple first-approximation model based on the Fuoss approach to ion-pair formation in electrolyte solutions.[19] Here, we consider the following association equilibrium in a charged membrane.

$$A + -\alpha X \overset{K_A}{\rightleftharpoons} AX_{-\alpha}$$

$$K_A = \frac{[AX_{-\alpha}]}{[A][X]^{-\alpha}} = \frac{\dfrac{C_{Xm} - \bar{C}_{Xm}}{(-\alpha)}}{\bar{C}_{1m}\bar{C}_{Xm}{}^{(-\alpha)}} \quad (1)$$

where X and A represent fixed-charge groups and counterions, respectively, $\alpha \equiv z_1/z_X$, and z_i is the valence of the ith species ($i = 1$ for a counterion, $i = 2$ for a co-ion, and $i = X$ for a fixed-charge group). The valence of the fixed-charge groups in the membrane, z_X, is $+1$ or -1.

According to the Fuoss formalism, the association constant between the fixed-charge groups and the counterions is expressed by

$$K_A = \frac{4\pi N_A a^3}{3 \times 10^{-3}} \times \exp\left[\frac{-z_1 z_X q^2}{4\pi\epsilon_v\epsilon_r a k_B T}\left(1 - \frac{z_1 + z_X}{2z_X}\frac{\kappa a}{1+\kappa a}\right)\right](-\alpha)^{\alpha}(\bar{C}_{1m})^{1+\alpha} \quad (2)$$

where N_A is Avogadro's number, a is the center-to-center distance between a fixed-charge group and a counterion, q is the electronic charge, ϵ_v and ϵ_r are the dielectric constant of a vacuum and the solvent, respectively, k_B is the Boltzmann constant, T is the absolute temperature, κ is the reciprocal of the Debye−Hückel length, and $\bar{C}_{1m}$ is the concentration of counterions in the membrane.

2.2. Membrane Potential. A charged membrane, thickness d, separates the same electrolyte solutions with different concentrations. $\bar{C}_{im}(x)$ represents the concentration of the ith species at coordinate x within the membrane. C_{iL} and C_{iR} denote the concentrations of the ith species in the bulk electrolyte solutions for the left-side cell and the right-side cell, respectively. According to the studies of Teorell, Meyer, and Sievers,[20] the membrane potential, $\Delta\phi$, is the sum of the Donnan potential at the left and right membrane−solution interfaces, $\Delta\phi_{Don}(L)$ and $\Delta\phi_{Don}(R)$, respectively, and the diffusion potential in the membrane, $\Delta\phi_{dif}$.

$$\Delta\phi = \Delta\phi_{Don}(L) + \Delta\phi_{dif} + \Delta\phi_{Don}(R) \quad (3)$$

2.2.1. Donnan Potential. The Donnan potentials at the left and right interfaces, $\Delta\phi_{Don}(L)$ and $\Delta\phi_{Don}(R)$, respectively, are written as follows[1]

$$\Delta\phi_{Don}(L) = \bar{\phi}_m - \phi_L = -\frac{RT}{z_i F}\ln\frac{\bar{\gamma}_{im}\bar{C}_{im}(0)}{k_i C_{iL}} \quad (4a)$$

$$\Delta\phi_{Don}(R) = \bar{\phi}_m - \phi_R = -\frac{RT}{z_i F}\ln\frac{\bar{\gamma}_{im}\bar{C}_{im}(d)}{k_i C_{iR}} \quad (4b)$$

where, $\bar{\gamma}_{im}$ is the ion activity coefficient of the ith species in the membrane and k_i is the partition coefficient of the ith species. The condition of electroneutrality in the membrane and in the bulk electrolyte solutions requires that

$$z_1\bar{C}_{1m} + z_2\bar{C}_{2m} + z_X\bar{C}_{Xm} = 0 \quad (5)$$

$$z_1 C_{1j} = -z_2 C_{2j} = -z_1 z_2 C_{sj} \quad j = L, R \quad (6)$$

where C_{sj} is the salt concentration in the bulk electrolyte solutions.

According to eqs 4−6, the concentrations of cations and anions in the membrane at the left and right interfaces obey the following equations.

$$\bar{C}_{1m}(j)^{-z_2}\left\{\bar{C}_{1m}(j) + \frac{z_X}{z_1}\bar{C}_{Xm}(j)\right\}^{z_1} - \left(\frac{\bar{\gamma}_{1m}}{k_1}\right)^{z_2}\left(\frac{\bar{\gamma}_{2m}}{k_2}\right)^{-z_1}(z_2 C_{sj})^{z_1 - z_2} = 0 \quad j = L, R \quad (7a)$$

$$\bar{C}_{2m}(j)^{z_1}\left\{\bar{C}_{2m}(j) + \frac{z_X}{z_2}\bar{C}_{Xm}(j)\right\}^{-z_2} - \left(\frac{\bar{\gamma}_{1m}}{k_1}\right)^{z_2}\left(\frac{\bar{\gamma}_{2m}}{k_2}\right)^{-z_1}(-z_1 C_{sj})^{z_1 - z_2} = 0 \quad j = L, R \quad (7b)$$

2.2.2. Diffusion Potential. The ionic flux across the membrane is given by the Nernst−Planck equation, which can be applied to the membrane phase

$$J_i = -\bar{D}_{im}\left(\frac{d\bar{C}_{im}}{dx} + z_i\bar{C}_{im}\frac{F}{RT}\frac{d\bar{\phi}_m}{dx}\right) \quad (8)$$

where J_i and $\bar{D}_{im}$ are the ionic flux and the diffusion coefficient of the ith species in the membrane.

By reordering eqs 2, 5, and 8, the following expressions are derived[1]

$$\frac{d\bar{\phi}_m}{dx} = \frac{\left(1 - \frac{z_2}{z_1}\right)\frac{d\bar{C}_{2m}}{dx} - \frac{1}{\alpha}\frac{d\bar{C}_{Xm}}{dx} + \frac{J_1}{\bar{D}_{1m}} + \frac{J_2}{\bar{D}_{2m}}}{\frac{F}{RT}z_X\bar{C}_{Xm}} \quad (9)$$

$$\frac{d\bar{C}_{2m}}{dx} = \frac{JI\frac{dC_{Xm}}{dx} + K}{1 - JH} \quad (10)$$

where

$$H = \frac{1 - BF}{A + BG} \quad (11)$$

$$I = \frac{-C}{A + BG} \quad (12)$$

$$J = \frac{\frac{z_2}{\alpha}\bar{C}_{2m}}{z_2\bar{C}_{2m}\left(1 - \frac{z_2}{z_1}\right) + z_X\bar{C}_{Xm}} \quad (13)$$

$$K = \frac{-z_2\bar{C}_{2m}\left(\frac{J_1}{\bar{D}_1} + \frac{J_2}{\bar{D}_2}\right) - z_X\bar{C}_{Xm}\frac{J_2}{\bar{D}_2}}{z_2\bar{C}_{2m}\left(1 - \frac{z_2}{z_1}\right) + z_X\bar{C}_{Xm}} \quad (14)$$

$$A = -\frac{1}{\beta}\left[1 + \frac{1}{K_A}\bar{C}_{Xm}^{(\alpha-1)}\{(1+\alpha)\bar{C}_{Xm} - \alpha C_{Xm}\}\right] \quad (15)$$

$$\beta \equiv \frac{z_2}{z_X}$$

$$B = \frac{1}{K_A{}^2}\frac{\bar{C}_{Xm}^{\alpha}}{\beta}[\bar{C}_{Xm} - C_{Xm}] \quad (16)$$

$$C = \frac{1}{K_A}\frac{\bar{C}_{Xm}^{\alpha}}{\beta} \quad (17)$$

$$F = K_A\left[\bar{C}_{1m}\frac{z_X + z_1}{2z_X}\frac{a}{(1+\kappa a)^2}\frac{z_1 z_X q^2}{4\pi\epsilon_v\epsilon_r a k_B T}D - z_2\bar{C}_{1m}{}^{-1}\left(\frac{1}{z_1} + \frac{1}{z_X}\right)\right] \quad (18)$$

$$G = K_A\left[\frac{z_X + z_1}{2z_X}\frac{a}{(1+\kappa a)^2}\frac{z_1 z_X q^2}{4\pi\epsilon_v\epsilon_r a k_B T}E - \bar{C}_{1m}{}^{-1}\left(1 + \frac{z_X}{z_1}\right)\right] \quad (19)$$

To obtain the ionic concentration and the electric potential profile in the membrane, eqs 9 and 10 must be solved using eqs 7a and 7b as boundary conditions. We have employed the following iterative procedure:

(i) We assumed an arbitrary value for the flux of the counterions, J_1. The flux of the co-ions, J_2, can be calculated as $J_2 = -z_1 J_1/z_2$, under the condition that the total current in the membrane is zero.

(ii) Equation 10 was solved using the modified Eular method with the boundary conditions at the left interface.

(iii) We examined the boundary conditions at the right interface. The initial value of the flux of counterions was changed, and the numerical calculation was repeated until the solution satisfied the boundary conditions at the right interface.

We can then obtain the electric potential profile within the membrane to integrate eq 9. The diffusion potential in the membrane, $\Delta\phi_{dif}$, is calculated as

$$\Delta\phi_{dif} = \bar{\phi}_m(R) - \bar{\phi}_m(L) \quad (20)$$

3. Experimental Section

3.1. Materials. Styrene monomer (St), 4-vinylpyridine (4VP), 55% divinylbenzene (DVB, mixture of isomers), sulfuric acid, methanol, *N*-methyl-2-pyrrolidone (NMP), and *n*-hexane were purchased from Wako Pure Chemical, Japan. Iodomethane was obtained from Kishida Chemical, Japan. *tert*-Butylperoxy-2-ethylhexanoate was purchased from NOF Corporation, Japan. These reagents were of extra-pure grade or for chemical use. High-density polyethylene (PE) porous membranes (Hipore H-4050U3, 50 μm thick and 0.2 μm average pore size) were obtained from Asahi Kasei Corporation, Japan.

3.2. Membrane Preparation. Three kinds of cation-exchange membranes (CEMs) with different water contents, composed of poly(styrene-*co*-divinylbenzene) (poly(St-*co*-DVB)) containing sulfonic acid groups, and three kinds of anion-exchange membranes (AEMs) with different water contents, composed of poly(styrene-*co*-4-vinylpyridine-*co*-divinylbenzene) (poly(St-*co*-4VP-*co*-DVB)) containing quaternary pyridinium groups, were prepared by radical copolymerization,[21] as previously reported.[2,3] The PE porous membranes were used as reinforcement for the charged membranes. The PE membranes (area = 4 × 4 cm^2) were soaked in MeOH for 24 h and vacuum-dried at room temperature. They were immersed in the monomer solutions, which were composed of St, DVB, and polymerization initiator (*tert*-butylperoxy-2-ethylhexanoate) for CEMs and St, 4VP, DVB, and the initiator for AEMs, under reduced pressure. The membranes containing monomer solution were placed between two poly(ethylene terephthalate) (PET) films and heated in a hot press at 70 °C for 32 h to form the base membranes. The poly(St-*co*-DVB) membranes were soaked in NMP for 30 min at room temperature and then sulfonated with 95% H_2SO_4. The poly(St-*co*-4VP-*co*-DVB) membranes were quaternized with 40 wt % CH_3I/*n*-hexane solution shielded from light at 40 °C for 20 h. The prepared membranes were washed thoroughly with MeOH and deionized water.

TABLE 1: Physicochemical Properties of Charged Membranes[a]

membrane	w_w (w/w %)	IEC (mmol/g of dry membrane)	C_X (mol/L)	thickness (μm)
CEM-1	6.7	0.62	8.6	50
CEM-2	15	1.5	8.5	50
CEM-3	40	2.9	4.2	50
Aciplex K501	30	1.5	5.5	170
AEM-1	9.0	0.58	5.9	50
AEM-2	11	0.71	5.6	50
AEM-3	22	0.77	2.7	50
Aciplex A501	26	1.4	5.4	140

[a] w_w, water content; IEC, ion-exchange capacity; C_X, fixed-charge density. Aciplex K501/A501, commercial CEM and AEM, respectively, are from Asahi Kasei Corporation, Japan.

3.3. Potentiometric Titration and Measurement of Equilibrium Water Content. The potentiometric titration was performed with an automatic titrator (DMS Titrino 716, Metrohm, Switzerland) as previously described.[2,3] A combined pH glass electrode (model no. 6.0218.010, Metrohm, Switzerland) and a combined Ag electrode (model no. 6.0450.100, Metrohm, Switzerland) were used for the titration of CEMs and AEMs, respectively. Two pieces of CEMs and AEMs (each membrane area was 4 × 4 cm^2) were immersed in 2 mol/L HCl and 2 mol/L KCl for 12 h to convert the counterion to the H^+ and Cl^- form, respectively. They were then washed sufficiently with deionized water. Thereafter, the CEMs were immersed in 50 mL of 2 mol/L KCl with stirring under N_2 gas flow for 1 h, and the AEMs were immersed in 50 mL of 2 mol/L $NaNO_3$ with stirring for 1 h. These treatments were repeated four times to elute H^+ or Cl^- thoroughly from the membranes, and all eluents were collected. The collected solutions were titrated with 0.1 mol/L KOH and 0.1 mol/L $AgNO_3$, respectively. The titers of KOH and $AgNO_3$ correspond to the amount of fixed-charge groups in the CEM and AEM, respectively, N_X (mol). The weight of the equilibrium swollen membrane, w_{wet} (g), was measured after carefully removing the surface water with filter paper, and the weight of dried membrane, w_{dry} (g), was measured after vacuum-drying at 100 °C for 6 h. The equilibrium water content of the membranes, w_w (%), is given by

$$w_w = \frac{w_{wet} - w_{dry}}{w_{wet}} \times 100 \quad (21)$$

The ion-exchange capacity, IEC (mol/g of dry membrane), and the fixed-charge density, C_X (mol/L), are determined by the following equations

$$\mathrm{IEC} = \frac{N_X}{w_{dry}} \tag{22}$$

$$C_X = \frac{\rho N_X}{w_{wet} - w_{dry}} \tag{23}$$

where ρ is density of water at 25 °C (0.99704×10^3 g/L).

All measurements were carried out at 25 ± 1 °C.

3.4. Energy-Dispersive X-Ray Analysis. The energy-dispersive X-ray (EDX) analysis detector (EDAX-PV9900, Philips, The Netherlands) of a field-emission scanning electron microscope (FE-SEM, S-800S, Hitachi, Japan) was used to characterize the distribution of fixed-charge groups across the prepared membranes.[2,3] According to the EDX elemental analysis of sulfur atoms and bromine atoms (counterions of the AEMs) along the membrane thickness, the respective distributions of sulfonic acid groups and quaternary pyridinium groups inside the membrane were monitored. All samples were coated with carbon.

3.5. Membrane Potential Measurements. The experimental setup is the same as that previously mentioned.[2,3] A charged membrane was installed at the center of the measuring cell, which had two acrylic containers, one on either side of the membrane. Both containers were filled with the electrolyte solutions of different concentrations; the right container was fixed at 0.001 mol/L, while the left one was varied from 0.001 to 3 mol/L. KCl, NaCl, LiCl, $CaCl_2$, and $MgCl_2$ were used for the measurements of CEMs. NaCl, NaBr, NaI, $NaNO_3$, and Na_2SO_4 were used for the measurements of AEMs. All measurements were carried out at 25 ± 0.5 °C.

3.6. Hydraulic Permeability Measurements. Hydraulic permeability of the membranes was obtained by measuring the transport volume of deionized water across the membranes for 10 min under an appropriate applied hydrostatic pressure. The applied pressure was varied from 0.1 to 3 MPa, and the membrane area exposed to the flow was 3.9 cm^2.

4. Results and Discussion

4.1. Membrane Preparation. The physicochemical properties of the prepared membranes are summarized in Table 1. Aciplex K-501/A-501 (Asahi Kasei Corporation, Japan) commercial hydrocarbon ion-exchange membranes were used for comparison. We succeeded in preparing charged membranes with various water contents by radical copolymerization, particularly low-water-content charged membranes, whose water contents are smaller than 10 wt %.

Figure 2 shows the typical charge distribution in the prepared membranes from the S Kα rays and Br Lα rays of the EDX analysis for (a) CEM and (b) AEM, respectively. This suggested that the fixed-charge groups, sulfonic acid groups, and quaternary pyridinium groups were homogeneously distributed in the CEM and AEM, respectively. The EDX analyses revealed that all of the prepared membranes have a homogeneous charge distribution.

4.2. Membrane Potential. A theoretical prediction of membrane potentials was performed based on our theoretical model. (Details of the calculation are described in the Theoretical Background section.) Before the calculation of membrane potentials, we estimated (i) the partition coefficients of ions between the membrane phase and the external electrolyte solution phase and (ii) the diffusion coefficients of ions in the membranes. The partition coefficients of the ions could not be obtained experimentally; therefore, we adapted Ferry's statistical calculation of partition coefficient, k_i, based on the assumptions that (i) the solutes are spherical and the pores are cylindrical and (ii) the interaction between the membrane matrix and a solute molecule is negligible.[22]

$$k_i = (1 - r_i/r_{pore})^2 \tag{24}$$

where r_i is the ionic radius of the ith species and r_{pore} is the pore radius of the membrane. (The crystallographic radius in ref 23 used as the ionic radius is listed in Table 2.) Here, we estimated the pore radius of the membrane by water permeability measurements using the Hagen−Poiseuille equation. (Actually, the prepared membranes appear to have a dense structure. Pusch, however, adapted this treatment for fine-porous synthetic membranes and estimated the mean pore radii within several nanometers.[24])

$$J_v = \frac{\theta r_{pore}^{\ 2}}{8\eta\tau}\frac{\Delta P}{\Delta x} \tag{25}$$

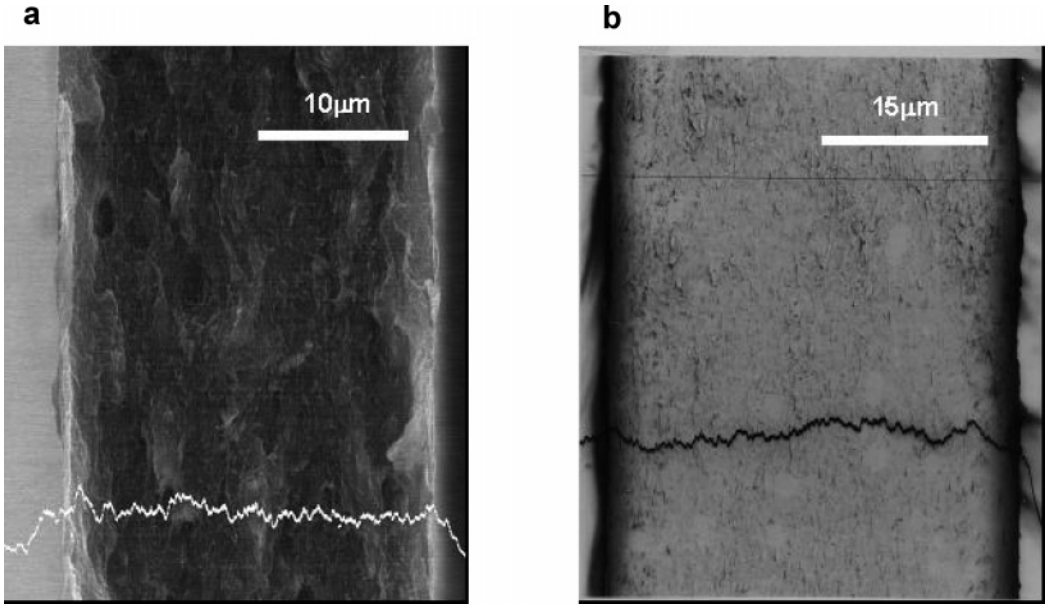

Figure 2. Fixed-charge distribution in charged membranes. (a) Cross-sectional SEM image of CEM-1 with the intensity of the S Kα rays from the EDX analysis. (b) Cross-sectional SEM image of AEM-1 with the intensity of the Br Lα rays from the EDX analysis.

TABLE 2: Crystallographic and Hydrated Radii of the Ions

	K^+	Na^+	Li^+	Mg^{2+}	Ca^{2+}	$N(CH_3)_4^+$	Cl^-	Br^-	I^-	NO_3^-	SO_4^{2-}
r_c (Å)	1.33	0.95	0.6	0.99	0.65	3.47	1.81	1.95	2.16	2.64	2.9
r_h (Å)	3.3	3.6	3.8	4.1	4.3	3.7	3.3	3.3	3.3	3.4	3.8

TABLE 3: Mean Pore Radius and Partition Coefficients of the Membranes

membrane	r_{pore} (nm)	k_{K^+}	k_{Na^+}	k_{Li^+}	$k_{Ca^{2+}}$	$k_{Mg^{2+}}$	k_{Cl^-}
CEM-1	1.2	0.56	0.51	0.49	0.45	0.43	0.49
CEM-2	1.6	0.64	0.61	0.59	0.56	0.55	0.59
CEM-3	2.4	0.74	0.72	0.71	0.69	0.67	0.71

membrane	r_{pore} (nm)	k_{Cl^-}	k_{Br^-}	k_{I^-}	$k_{NO_3^-}$	$k_{SO_4^{2-}}$	k_{Na+}
AEM-1	1.3	0.57	0.57	0.57	0.56	0.51	0.53
AEM-2	1.4	0.58	0.58	0.58	0.57	0.53	0.55
AEM-3	1.8	0.67	0.67	0.67	0.66	0.62	0.64

where J_v is the flux of water, η is the viscosity of water, ΔP is the pressure difference, Δx is the membrane thickness, θ is the porosity of the membrane (θ = (water volume)/(membrane volume)), and τ is the tortuosity factor of the membrane ($\tau = (2-\theta)/\theta$).[25] The mean pore radius and the partition coefficients of the membranes are listed in Table 3. The diffusion coefficient of ions in the membranes was given by

$$\bar{D}_{im} = \frac{D_i}{\tau^2} \tag{26}$$

where $\bar{D}_{im}$ and D_i represent the diffusion coefficient of the ith species in the membrane and that in the solution, respectively. The diffusion coefficients of the ions in the bulk water are summarized in Table 4.[26]

The theoretical calculations of membrane potentials were fitted to the experimental data. Here, the dielectric constant in the membrane, ϵ_r, and the center-to-center distance of the ion pair, a, are the fitting parameters with the following conditions

$$2 < \epsilon_r < 78 \tag{27}$$

$$r_c^c < a < r_h^c + r_h^f \tag{28}$$

where r_c^c, r_h^c, and r_h^f are the crystallographic radius of the counterion, hydrated radius of the counterion, and hydrated radius of the fixed-charge group, respectively. The values of the dielectric constants, 2 and 78, correspond to that of the bulk polymer of the membrane matrix, poly(St-*co*-DVB), and bulk water, respectively. We assumed that the center-to-center distance of the ion pair changed from the crystallographic radius of the counterion to the sum of the hydrated radii of the fixed-charge group and the counterion. The sizes of ions used in the calculation are summarized in Table 2.[23] We used the hydrated radii of SO_4^{2-} and $N(CH_3)_4^+$ as those of fixed-charge groups of the CEMs and AEMs, respectively, for approximation. In the calculations, the ion activity coefficient in the external electrolyte solution was used as that in the membrane.

Figure 3 shows the typical experimental results for the membrane potential for (a) CEM and (b) AEM. The points and solid lines represent the experimental data and the theoretical results, respectively. All the calculated results of the membrane potential agreed well with the experimental values. This supported the belief that the ion-pairing effect was substantial in a low-water-content membrane system. In the following section, we examine the fitting parameters, ϵ_r and a, obtained from our theoretical analysis.

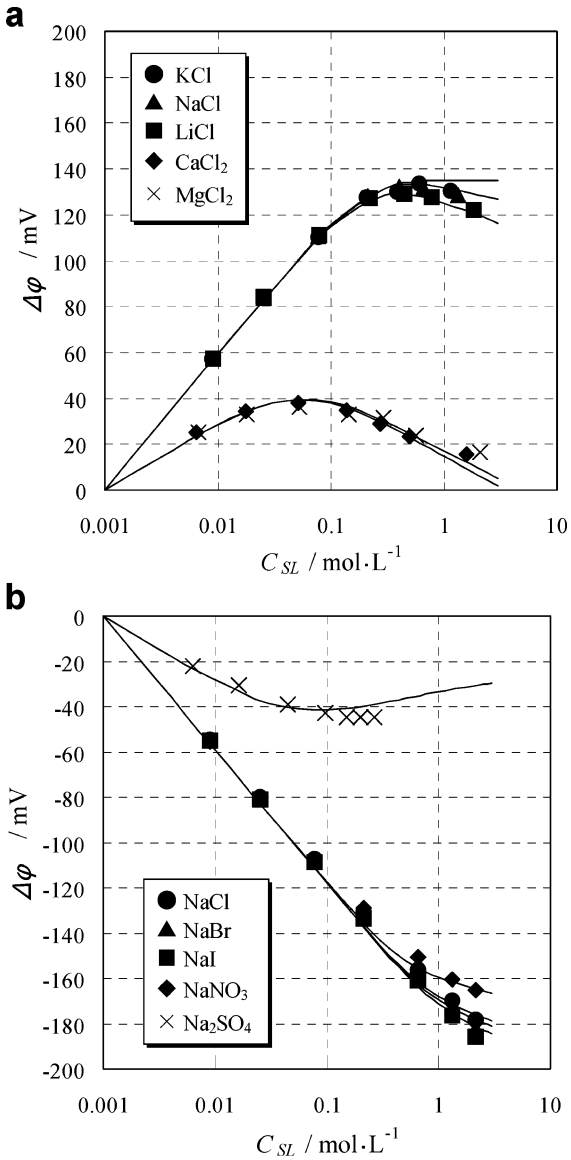

Figure 3. Membrane potential across the membranes as a function of electrolyte concentration in the bulk solutions (C_{SL}): (a) CEM-2; (b) AEM-2. Solid lines indicate the theoretical results obtained by fitting our theory considering ion-pair formation between fixed-charge groups and counterions to the experimental data.

4.3. Dielectric Constant in the Membranes and Center-to-Center Distance of an Ion Pair. Figure 4 and Table 5, respectively, demonstrate the water-content dependence of the dielectric constant, ϵ_r, in the membranes and the center-to-center distance of an ion pair, a, based on our theoretical analysis. As can be seen in Figure 4, the dielectric constant in the membranes is smaller than the value in the bulk water ($\epsilon_r = 78$). Table 5

TABLE 4: Diffusion Coefficients of the Ions in the Bulk Water

	K^+	Na^+	Li^+	Mg^{2+}	Ca^{2+}	Cl^-	Br^-	I^-	NO_3^-	SO_4^{2-}
D ($\times 10^5$ cm^2/s)	1.957	1.334	1.030	0.7922	0.7063	2.033	2.081	2.046	1.903	1.065

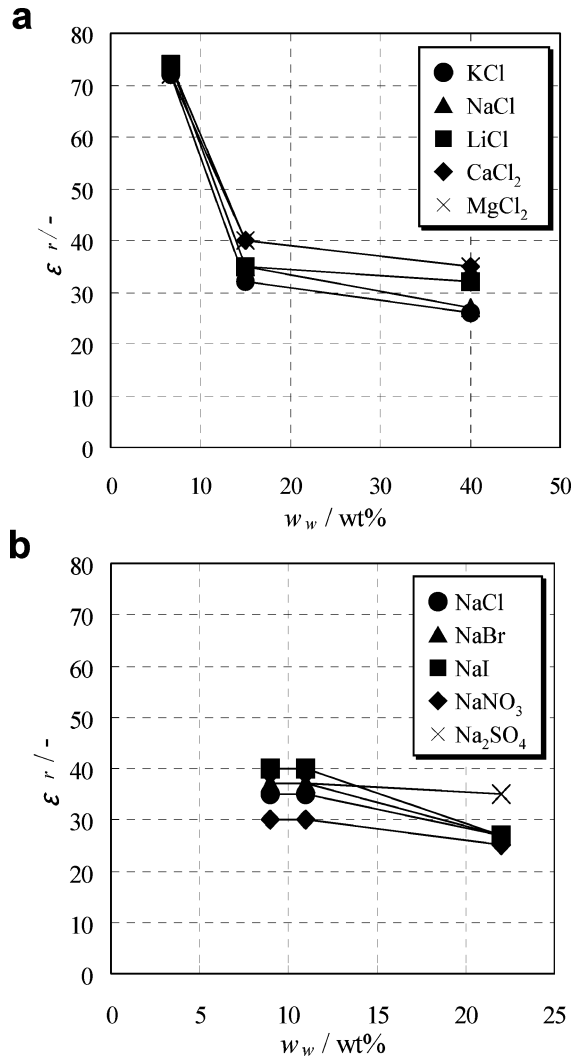

Figure 4. Dielectric constants in the membranes, ϵ_r, as a function of the water content from the theoretical analysis: (a) CEMs; (b) AEMs.

TABLE 5: Center-to-Center Distances of Ion Pairs in the Membranes from Theoretical Calculations

	a (Å)				
membrane	K^+	Na^+	Li^+	Ca^{2+}	Mg^{2+}
CEM-1	1.8	1.6	2.2	3.3	3.4
CEM-2	1.8	1.7	1.7	3.6	3.7
CEM-3	1.8	1.7	1.5	3.7	3.7

	a (Å)				
membrane	Cl^-	Br^-	I^-	NO_3^-	SO_4^{2-}
AEM-1	3	2.9	3.0	2.8	3.3
AEM-2	3	2.9	3.0	2.8	3.5
AEM-3	2.6	2.6	3.0	2.8	3.5

indicates that the center-to-center distance of an ion pair is independent of the water content of the membranes and within the range from the crystallographic radius to the hydrated radius of a counterion (Table 2). These results suggested that fixed-charge groups in the membrane were neutralized by associated counterions. This is attributed to dielectric saturation. Water-content dependences of the dielectric constant showed a different behavior between CEMs and AEMs: The dielectric constant in a CEM remarkably increased with a decrease in the water content of around 10 wt %, while that in an AEM did not show a water-content dependence. This interesting behavior of the dielectric constant for a CEM contradicts the general prediction that the dielectric constant in a low-water-constant membrane would be low due to dielectric saturation.[1] For the sulfonated poly(St-*co*-DVB) membranes, however, Tasaka et al. reported that the amount of nonfreezing water in the membrane, whose mobility is strongly restricted by the interactions between the polymer matrix and a water molecule, decreased with a decrease in the water content based on their differential scanning calorimetry measurements.[27] Under such a condition, it is presumed that the dielectric constant in the membrane increased with a decrease in the water content.

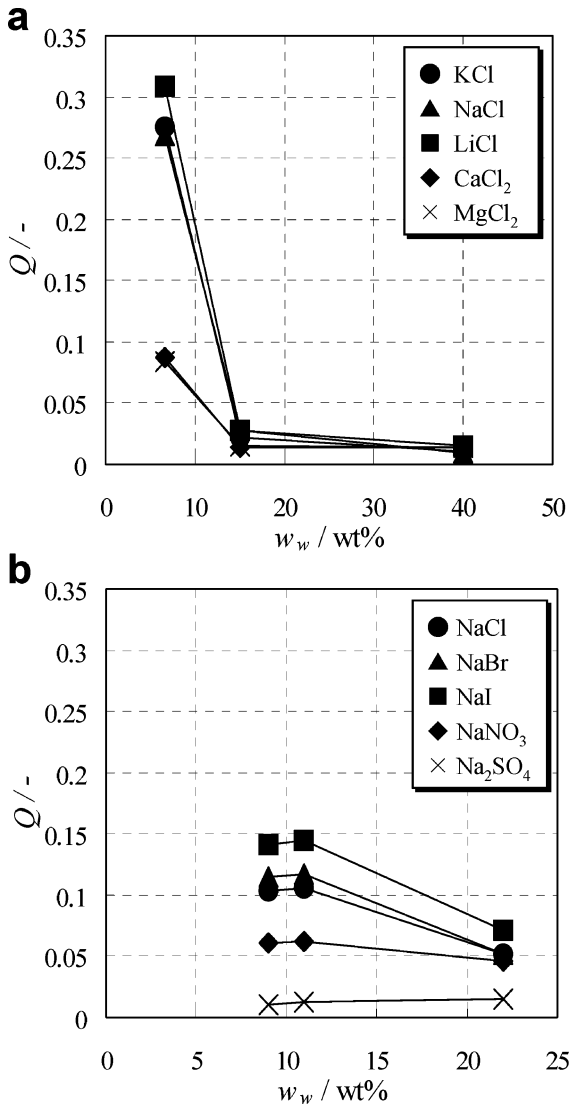

Figure 5. Charge effectiveness of the membranes, *Q*, as a function of the water content: (a) CEMs; (b) AEMs

4.4. Charge Effectiveness of the Membranes. All of the fixed-charge groups in the membrane do not function perfectly due to the neutralization by the counterion. Therefore, the effectiveness of fixed-charge groups in the membrane is an important index for the discussion of the ionic transport phenomenon across charged membranes. The charge effectiveness of the membrane, *Q*, represents the effectiveness of the fixed-charge groups in the membranes and is defined as follows

$$Q = \frac{\frac{1}{d}\int_0^d \bar{C}_{\mathrm{Xm}}(x)\,\mathrm{d}x}{C_{\mathrm{Xm}}} \tag{29}$$

Figure 5 shows the charge effectiveness of the membranes as a function of water content of the membranes. The charge

effectiveness of the membranes was small (<0.35). The water-content dependence of the charge effectiveness of the membrane obeyed that of the dielectric constants in the membranes: The charge effectiveness of the CEM showed a critical point around 10 wt % water content. (This result implies that charged membranes may show large charge effectiveness and high permselectivity even under the low-water-content condition.) The charge effectiveness of the membrane in a divalent counterion system ($MgCl_2$ and $CaCl_2$ for CEMs; Na_2SO_4 for AEMs) was much lower than that in a monovalent counterion system. This phenomenon can also be explained by the ion-pairing effect: The electrostatic interaction between a fixed-charge group and a counterion depends on the valence of the counterions.[1]

5. Conclusions

In the present study, we verified the ion-pairing effect in low-water-content charged membranes based on membrane potential measurements. The experimental results were analyzed based on the Donnan equilibrium, the Nernst−Planck equation for ion flux, and the Fuoss formalism for ion-pair formation between the fixed-charge groups and counterions in the membranes. The theoretical predictions agreed well with the experimental results. This showed that the ion-pairing effect was substantial in the low-water-content membrane system. Our first-approximation theoretical approach also revealed the following findings: (i) Dielectric constants in the membrane were smaller than the value in bulk water. The dielectric constant in the CEM showed a critical point near 10 wt % water content while that in the AEM did not show a water-content dependence. (ii) The center-to-center distance of an ion pair was independent of the water content of the membranes. (iii) The charge effectiveness of the membrane was small (<0.35). The water-content dependence of the charge effectiveness of the membranes obeyed that of the dielectric constants in the membrane. These results provide fundamental knowledge for the development of not only polyelectrolyte membranes for fuel cells but also high-performance membranes for other applications. Recently, Okada et al. also studied the local structure of counterions in ion-exchange resins by X-ray absorption fine structure (XAFS) spectroscopy.[28] They evaluated the direct ion pairs between the fixed-charge groups and counterions. A more detailed discussion on ion-pairing in the membranes based on both membrane potential measurements and other spectroscopic measurements (e.g., XAFS, NMR, dielectric relaxation measurements in the GHz region,[29] and so forth) will be required.

Acknowledgment. The authors express appreciation to Mr. Hamada and Mr. Kinoshita, Asahi Kasei Corporation, for kindly providing PE porous membranes and commercial ion-exchange membranes. This work was partly supported by the Research and Development Program for Polymer Electrolyte Fuel Cells from the New Energy and Industrial Technology Development Organization, NEDO, Japan.

Supporting Information Available: Composition of the monomer solution and sulfonation conditions for CEMs, composition of the monomer solution for AEMs, and porosity and tortuosity factors of charged membranes. This material is available free of charge via the Internet at http://pubs.acs.org.

References and Notes

(1) Yamamoto, R.; Matsumoto, H.; Tanioka, A. *J. Phys. Chem. B* **2003**, *107*, 10615.
(2) Yamamoto, R.; Matsumoto, H.; Tanioka, A. *J. Phys. Chem. B* **2003**, *107*, 10506.
(3) Tanioka, A.; Matsumoto, H.; Yamamoto, R. *Sci. Technol. Adv. Mater.* **2004**, *5*, 461.
(4) Saito, K.; Tanioka, A.; Miyasaka, K. *Polymer* **1994**, *35*, 5098.
(5) Kawaguchi, M.; Murata, T.; Tanioka, A. *J. Chem. Soc., Faraday Trans.* **1997**, *93*, 1351.
(6) Matsumoto, H.; Tanioka, A.; Murata, T.; Higa, M.; Horiuchi, K. *J. Phys. Chem. B* **1998**, *102*, 5011.
(7) Glueckauf, E.; Watts, R. E. *Proc. R. Soc. London, Ser. A* **1962**, *268*, 339.
(8) Glueckauf, E. *Proc. R. Soc. London, Ser. A* **1962**, *268*, 350.
(9) Reiss, H.; Bassignana, I. C. *J. Membr. Sci.* **1982**, *11*, 219.
(10) Selvey, C.; Reiss, H. *J. Membr. Sci.* **1985**, *23*, 11.
(11) Petropoulos, J. H.; Tsimboukis, D. G.; Kouzeli, K. *J. Membr. Sci.* **1983**, *16*, 379.
(12) Petropoulos, J. H. *J. Membr. Sci.* **1990**, *52*, 305.
(13) Larter, R. *J. Membr. Sci.* **1986**, *28*, 165.
(14) Mafé, S.; Ramírez, P.; Tanioka, A.; Pellicer, J. *J. Phys. Chem. B* **1997**, *101*, 1851.
(15) Chou, T.-J.; Tanioka, A. *J. Membr. Sci.* **1998**, *144*, 275.
(16) Chou, T.-J.; Tanioka, A. *J. Phys. Chem. B* **1998**, *102*, 129.
(17) Chou, T.-J.; Tanioka, A. *J. Phys. Chem. B* **1998**, *102*, 7198.
(18) Chou, T.-J.; Tanioka, A. *J. Phys. Chem. B* **1998**, *102*, 7866.
(19) Fuoss, R. M. *J. Am. Chem. Soc.* **1958**, *80*, 5059.
(20) Lakshiminarayanaiah, N. *Transport Phenomena in Membranes*; Academic Press: New York, 1969.
(21) Mizutani, Y. *Kogyo Kagaku Zasshi* **1962**, *65*, 1124.
(22) Ferry, J. D. *J. Gen. Physiol.* **1936**, *20*, 95.
(23) Nightingale, E. R. *J. Phys. Chem.* **1959**, *63*, 1381.
(24) Pusch, W. In *Water Science Reviews 3: Water Dynamics*; Flanks, F., Ed.; Cambridge University Press: Cambridge, U. K.1988; p 297.
(25) Mackie, J. S.; Meares, P. *Proc. R. Soc. London, Ser. A* **1955**, *232*, 498.
(26) Robinson, R. A.; Stokes, R. H. *Electrolyte Solutions*, 2nd ed.; Butterworth: London, U. K., 1959; p 513−515.
(27) Tasaka, M.; Suzuki, S.; Ogawa, Y.; Kamaya, M. *J. Membr. Sci.* **1988**, *38*, 175.
(28) Harada, M.; Okada, T.; Watanabe, I. *J. Phys. Chem. B* **2002**, *106*, 34.
(29) Paddison, S. J.; Bender, G.; Kreuer, K. D.; Nicoloso, N.; Zawodzinski, T. A., Jr. *J. New Mater. Electrochem. Syst.* **2000**, *3*, 291.